

**Exchange interactions and Curie temperature in (Ga,Mn)As**

L. M. Sandratskii\* and P. Bruno

*Max-Planck Institut für Mikrostrukturphysik, D-06120 Halle, Germany*

(Received 28 June 2002; published 31 October 2002)

We use supercell and frozen-magnon approaches to study the dependence of the magnetic interactions in (Ga,Mn)As on the Mn concentration. We report the parameters of the exchange interaction between Mn spins and the estimates of the Curie temperature within the mean-field and random-phase approximations. In agreement with experiment we obtain a nonmonotonous dependence of the Curie temperature on the Mn concentration. We estimate the dependence of the Curie temperature on the concentration of the carries in the system and show that the decrease of the number of holes in the valence band leads to a fast decrease of the Curie temperature. We show that the hole states of the valence band are more efficient in mediating the exchange interaction between Mn spins than the electron states of the conduction band.

DOI: 10.1103/PhysRevB.66.134435

PACS number(s): 75.50.Pp, 75.30.Et, 71.15.Mb

**I. INTRODUCTION**

An important current problem on the way to the practical use of spin transport in semiconductor devices is the design of materials that make possible the injection of spin-polarized electrons into semiconductors at room temperature. One of the promising classes of materials is the diluted magnetic semiconductors (DMS's) of the III-V type. A strong interest in these systems was attracted by the observation of ferromagnetism in (GaMn)In (Ref. 1) and (GaMn)As (Ref. 2) with the Curie temperature of  $\text{Ga}_{0.947}\text{Mn}_{0.053}\text{As}$  as high as 110 K. To design material with a Curie temperature higher than room temperature knowledge of the physical mechanisms governing the exchange interactions in these systems is of primary importance.

The theoretical works on ferromagnetism in DMS systems can be separated into two groups. The first group models the problem with an effective Hamiltonian containing experimentally determined parameters. This part of the studies was recently reviewed in Refs. 3 and 4. This paper belongs to the second group of studies, which are based on parameter-free calculations within density functional theory. Several calculations have been performed recently along this line. In Refs. 5–7, the coherent potential approximation (CPA) was used to study the magnetic structure, density of states, total energy, and chemical trends in (III,Mn)V. In Refs. 8–11, the calculations were performed for a series of magnetic states of (III,Mn)V using supercells of zinc-blende structure and focusing basically on the same physical quantities as the CPA studies. Since the CPA is a single-site theory which neglects any short-range order in disordered subsystems, the CPA and supercell approaches are complementary. In Refs. 5, 7, and 10, the influence of the antisite defects on the magnetic properties of DMS's is discussed. In Ref. 11, the total energy of various collinear magnetic configurations is used to estimate the parameters of the exchange interaction between the  $3d$  atoms forming clusters in III-V semiconductors.

The purpose of the present paper is a parameter-free calculation of the exchange interactions and Curie temperature in (GaMn)As for various concentrations of Mn. The study is based on the supercell approach.

Density functional theory (DFT) has proved to be very successful in the parameter-free description of the ground-state magnetic properties of complex systems (see, e.g., Ref. 12). Recently much attention has been devoted to the application of the methods of DFT to studies of the low-energy excitations of magnetic systems and the magnetic phase transitions.<sup>13–21</sup> Stoner theory, which relates finite-temperature effects to the temperature variation of the Fermi-Dirac distribution, appeared to be unable to describe the temperature properties of the magnetic systems with itinerant electrons.<sup>22</sup> A necessary feature of the theoretical description of finite-temperature effects is an account of transversal fluctuations of the local magnetization. A most consequent method of the calculation of the low-energy magnetic excitations is based on evaluation of the nonuniform and frequency-dependent enhanced magnetic susceptibility.<sup>18</sup> This approach is, however, computationally very complicated and up to now has been successfully applied to the simplest magnetic systems only.

A more tractable approach to the study of both spin-wave excitations and the thermodynamics of magnetic systems is based on an adiabatic treatment of atomic magnetic moments.<sup>13–17,19–21</sup> In this approach an account of noncollinear configurations of atomic moments is essential. An effective method for estimation of the parameters of the interatomic exchange interaction and spin-wave energies is suggested by the frozen-magnon approach.<sup>16,21</sup> This approach is based on the total-energy calculation for spiral magnetic configurations. Because of the generalized translational periodicity of spin spirals,<sup>23</sup> such calculations can be performed very efficiently.<sup>24</sup> Additional help is provided by the force theorem<sup>13</sup> which allows to use the band energy of non-self-consistent frozen-magnon states for estimation of the total-energy differences. In the present paper this approach is used to study the exchange interactions and Curie temperature in  $\text{Ga}_{1-x}\text{Mn}_x\text{As}$  with various concentrations of Mn impurities.

**II. CALCULATIONAL SCHEME**

The calculations are based on the supercell approach where one of the Ga atoms in a supercell of zinc-blende

GaAs is replaced by the Mn atom. The concentration of Mn depends on the size of the supercell. The following concentrations  $x$  have been studied in this work: 0.25, 0.125, 0.0625, and 0.03125. For comparison, calculation of the density of states (DOS) of pure MnAs and GaAs is also performed. In order to better identify trends we investigate here a concentration range that is much wider than the one accessible to experiment so far.

The calculations were carried out with the augmented-spherical-wave (ASW) method.<sup>25</sup> In all calculations the lattice parameter was chosen to be equal to the experimental lattice parameter of GaAs. Two empty spheres per formula unit have been used in the calculations. The positions of the empty spheres are (0.5, 0.5, 0.5) and (0.75, 0.75, 0.75). Radii of all atomic spheres were chosen to be equal. Depending on the concentration of Mn, the supercell is cubic ( $x=25\%$ ,  $a \times a \times a$ , and  $x=3.125\%$ ,  $2a \times 2a \times 2a$ ) or tetragonal ( $x=12.5\%$ ,  $a \times a \times 2a$  and  $6.25\%$ ,  $2a \times 2a \times a$ ).

To describe the exchange interactions in the system we use an effective Heisenberg Hamiltonian of classical spins,

$$H_{eff} = - \sum_{i \neq j} J_{ij} \mathbf{e}_i \cdot \mathbf{e}_j, \quad (1)$$

where  $J_{ij}$  is an exchange interaction between two Mn sites ( $i, j$ ) and  $\mathbf{e}_i$  is the unit vector pointing in the direction of the magnetic moments at site  $i$ .

To estimate the parameters of the Mn-Mn exchange interaction we performed a calculation for the following frozen-magnon configurations:

$$\theta_i = \text{const}, \quad \phi_i = \mathbf{q} \cdot \mathbf{R}_i, \quad (2)$$

where  $\theta_i$  and  $\phi_i$  are the polar and azimuthal angles of vector  $\mathbf{e}_i$  and  $\mathbf{R}_i$  is the position of the  $i$ th Mn atom. The directions of the induced moments in the atomic spheres of Ga and As and in the empty spheres were kept parallel to the  $z$  axis.

It can be shown that within the Heisenberg model (1) the energy of such configurations can be represented in the form

$$E(\theta, \mathbf{q}) = E_0(\theta) - \frac{\theta^2}{2} J(\mathbf{q}), \quad (3)$$

where  $E_0$  does not depend on  $\mathbf{q}$  and  $J(\mathbf{q})$  is the Fourier transform of the parameters of the exchange interaction between pairs of Mn atoms:

$$J(\mathbf{q}) = \sum_{j \neq 0} J_{0j} \exp(i\mathbf{q} \cdot \mathbf{R}_{0j}). \quad (4)$$

In Eq. (3) the angle  $\theta$  is assumed to be small. Using  $J(\mathbf{q})$  one can estimate the energies of the spin-wave excitations:

$$\omega(\mathbf{q}) = \frac{4}{M} [J(\mathbf{0}) - J(\mathbf{q})] = \frac{8}{M\theta^2} [E(\theta, \mathbf{q}) - E(\theta, \mathbf{0})], \quad (5)$$

where  $M$  is the atomic moment of the Mn atom. Performing a back Fourier transformation we obtain the parameters of the exchange interaction between Mn atoms:

$$J_{0j} = \frac{1}{N} \sum_{\mathbf{q}} \exp(-i\mathbf{q} \cdot \mathbf{R}_{0j}) J(\mathbf{q}). \quad (6)$$

The calculation of  $E(\theta, \mathbf{q})$  for different Mn concentrations has been performed for uniform meshes in the first Brillouin zone (BZ) for  $\theta=30^\circ$ . The symmetry of the system was employed to reduce the amount of calculations. For cubic supercells (Mn concentrations 25% and 3.125%) the crystal structure possesses 24 point symmetry operations, and for the tetragonal unit cells (Mn concentrations 12.5% and 6.25%) the number of point operations is 8. Since the energy as a function of  $\mathbf{q}$ , is invariant with respect to the reversal of  $\mathbf{q}$  the irreducible part of the BZ is  $\frac{1}{48}$ th and  $\frac{1}{16}$ th correspondingly for cubic and tetragonal supercells.

The number and type of the exchange parameters determined in the back Fourier transformation with Eq. (6) are uniquely determined by the  $\mathbf{q}$  mesh. The parameters obtained in this procedure guarantee that  $J(\mathbf{q})$  calculated according to Eq. (4), reproduces exactly the calculated values of the total energy. The calculation for a more dense  $\mathbf{q}$  mesh gives additionally the parameters of the exchange interaction between more distant atoms.

The Curie temperature was estimated in the mean-field approximation (MFA)

$$k_B T_C^{MFA} = \frac{2}{3} \sum_{j \neq 0} J_{0j} = \frac{M}{6\mu_B} \frac{1}{N} \sum_{\mathbf{q}} \omega(\mathbf{q}) \quad (7)$$

and random phase approximation (RPA)

$$\frac{1}{k_B T_C^{RPA}} = \frac{6\mu_B}{M} \frac{1}{N} \sum_{\mathbf{q}} \frac{1}{\omega(\mathbf{q})}. \quad (8)$$

To evaluate the RPA value of the Curie temperature the  $\omega(\mathbf{q})$  was considered continuous in  $\mathbf{q}$  space. In a small sphere with the center at  $\mathbf{q}=0$  the singular function  $1/\omega(\mathbf{q})$  was approximated by the function  $1/Dq^2$  and then replaced by a continuous function which has the same value and slope at the sphere boundary. The difference between the singular and continuous functions was integrated analytically. The regular function obtained was integrated numerically.

Since the  $T_C^{MFA}$  and  $T_C^{RPA}$  are given by the arithmetic and harmonic averages of the spin-wave energies,  $T_C^{MFA}$  is always larger than  $T_C^{RPA}$ .<sup>20</sup> Physically this difference can be explained by an increased role of the low-energy excitations in the case of the RPA. In the case of the ferromagnetic 3d metals the RPA gives, in general, better agreement with experiment.<sup>20</sup>

### III. DENSITY OF STATES

We begin with a discussion of the trends in the variation of the electron DOS (Fig. 1). For all Mn concentrations studied there is an energy gap in the spin-down DOS in an energy interval containing the Fermi level or close to it. This gap is about 0.1 Ry in MnAs and decreases to a value of about 0.05 Ry for lower Mn content. In MnAs and  $\text{Ga}_{0.75}\text{Mn}_{0.25}\text{As}$ , the Fermi level is slightly above the gap. For MnAs, the energy distance between the Fermi level and

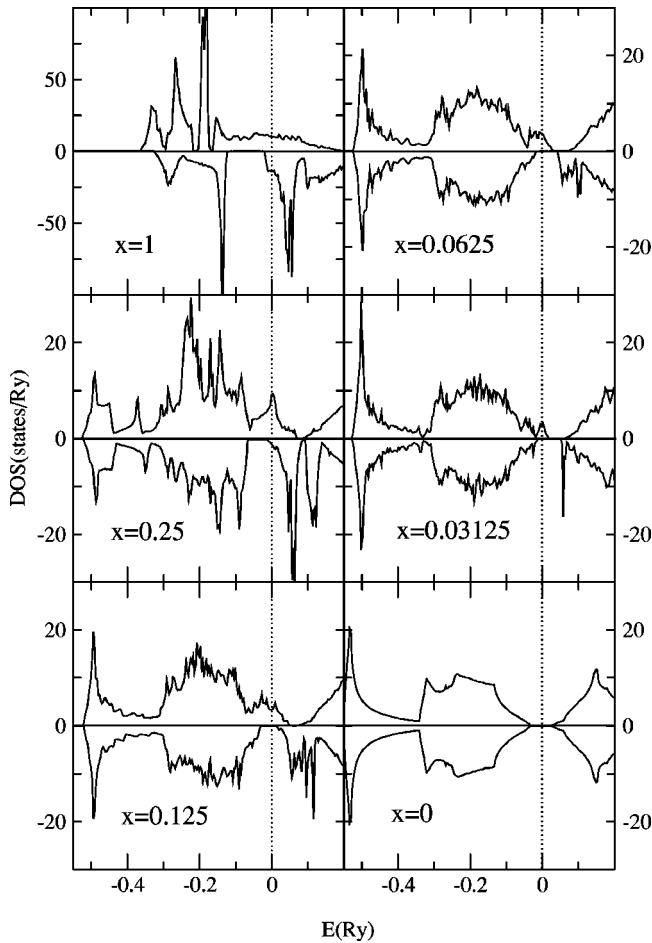


FIG. 1. The DOS of  $\text{Ga}_{1-x}\text{Mn}_x\text{As}$ . The DOS is given per unit cell of the zinc-blende crystal structure. The DOS above (below) the abscissas axis corresponds to the spin-up (-down) states.

upper edge of the gap is about 0.015 Ry. For  $x=0.25$ , this distance is less than 0.005 Ry. For lower Mn concentrations the Fermi level lies within the gap moving from the upper to the lower part of the gap with decreasing  $x$ . This means that for concentrations of Mn less than 25% the calculated ground state is half-metallic. This property is very important for efficient spin injection into semiconductor.<sup>26</sup> In the half-metallic ferromagnetic state the value of the magnetic moment per supercell is integer (Table I).

The situation with spin-up DOS is different. In MnAs there is no energy gap close to the Fermi level. For  $x$

TABLE I. Magnetic moments in  $\text{Ga}_{1-x}\text{Mn}_x\text{As}$ . There are shown the Mn moment, the induced moment on the nearest As atoms, and the magnetic moment of the unit cell (supercell in the case of  $x \neq 1$ ). All moments are in units of  $\mu_B$ .

	$x$				
	1	0.25	0.125	0.0625	0.03125
Mn	3.76	3.85	3.88	3.94	3.95
As	-0.18	-0.046	-0.046	-0.036	-0.032
Cell	3.65	3.98	4.00	4.00	4.00

$=0.25$  a small gap appears at the energy 0.07 Ry above the Fermi level. With decreasing  $x$ , this gap increases and its lower edge becomes closer to the Fermi level. At the Mn concentration of 6.25% there is an overlap of the spin-up and spin-down gaps and an energy gap appears in the total DOS. The gap in the total DOS can be treated as a gap between the valence and conduction bands of the system. The upper part of the valence band is not occupied and contains holes. The hole states are of the spin-up type.

Comparison of our DOS with the corresponding DOS available in the scientific literature shows good agreement. Thus, our DOS for the Mn concentration of 3.125% is close to the corresponding DOS from Ref. 9 calculated with the use of the pseudopotential approach. Also the partial DOS for  $x=6.25\%$  presented in Ref. 8 is in good agreement with the curves obtained in our calculations.

The values of the calculated moments in the Mn atomic sphere are collected in Table I and are close to  $4\mu_B$ . Similar values have been obtained in other calculations within the density functional theory (see, e.g., Refs. 8, 9, and 11). Taking as an example the system with  $x=3.125\%$  we find that the contribution of the 3d electrons into the Mn moment is  $3.83\mu_B$  with the rest  $0.12\mu_B$  coming from the 4s and 4p electrons. Note that the total number of the 3d electrons in the Mn sphere is 5.30. The difference between the number of the 3d electrons and their contribution into the spin moment results from the presence of 0.73 spin-down 3d electrons in the Mn atomic sphere (see the spin-down Mn-DOS in Fig. 2). The hybridization between the Mn 3d states and the states of the valence band of GaAs is crucial for the appearance of the occupied spin-down 3d states. In some model-Hamiltonian studies a physical picture is used which considers the Mn 3d electrons as strongly localized and forming an atomic spin of  $S=\frac{5}{2}$ . The density-functional-theory calculations show that this picture, although useful in qualitative studies, does not take into account some important features of the Mn 3d states.

One of the important issues in the magnetism of the DMS's is the spatial localization of the hole states. Comparison of the DOS of pure GaAs and the GaMnAs with  $x=3.125\%$  helps to get insight into the physical mechanism of the formation of the hole states. The replacement of one Ga atom in the supercell of GaAs by a Mn atom does not change the number of spin-down states in the valence band. In the spin-up channel there are, however, five additional energy bands which are related to the Mn 3d states. Since there are five extra energy bands and only four extra electrons (the atomic configurations of Ga and Mn are  $4s^24p^1$  and  $3d^54s^2$ ) the valence band is not filled and there appear unoccupied (hole) states at the top of the valence band. The integrated number of the hole states is exactly one hole per Mn atom (correspondingly, one hole per supercell). The distribution of the hole in the supercell for the Mn concentration of 3.125% is shown in Fig. 3. About 18.5% of the hole is in the Mn sphere, 22.5% in the first coordination sphere of the As atoms. Correspondingly about 60% of the hole is outside of the first coordination sphere of the impurity. About 58.3% of the hole is on the As atoms, 17.7% on Ga sites, 5.5% in the empty spheres. Thus, the hole states are rather delocal-

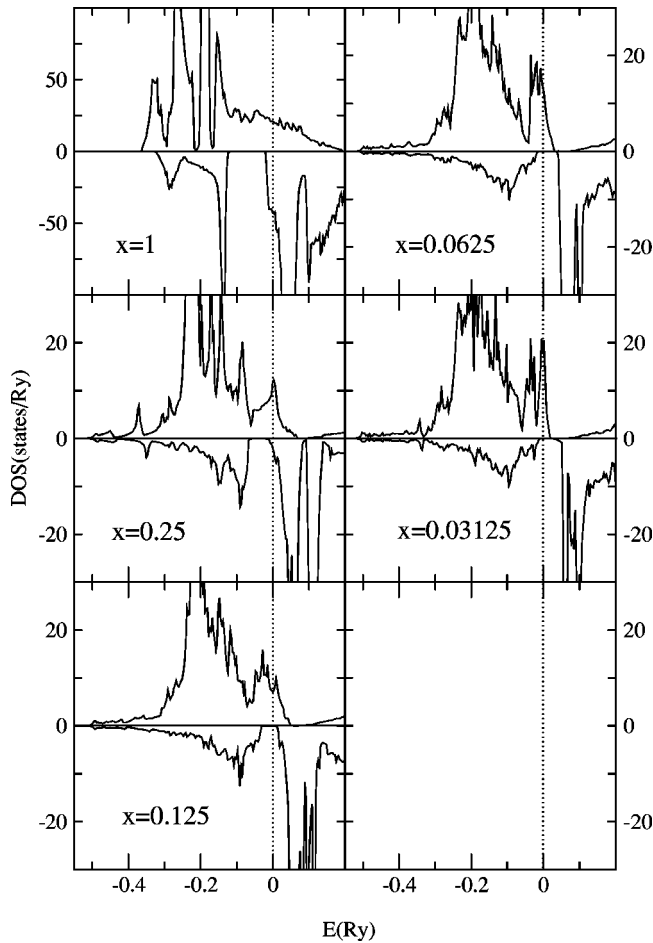


FIG. 2. The partial Mn-DOS for  $\text{Ga}_{1-x}\text{Mn}_x\text{As}$ . The DOS is given per Mn atom.

ized. Even the most distant As atom contains 4.5% of the hole. The delocalized character of the hole states is an important factor in mediating the exchange interaction between Mn atoms.

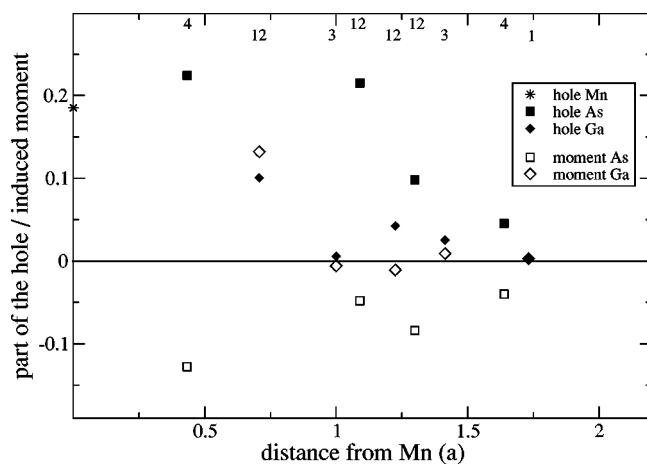


FIG. 3. Hole distribution and induced moments (in  $\mu_B$ ) for  $\text{Ga}_{1-x}\text{Mn}_x\text{As}$  with  $x=0.03125$ . All values are given for the coordination spheres. The numbers of atoms in the coordination spheres are given at the top of the picture.

Another important quantity characterizing the localization of the valence-band states about impurities is the values of the induced moments on various atoms. The values of the atomic moments for  $x=3.125\%$  are shown in Fig.3. It is seen that even at the As atom most distant from Mn impurities there is substantial spin polarization, which provides an efficient exchange path between Mn atoms. The dependence of the induced moment on the distance from Mn is nonmonotonous for both As and Ga. This behavior can be related to the spin density oscillation in Ruderman-Kittel-Kasuya-Yoshida (RKKY) theory. A detailed analysis of the formation of the induced atomic moments shows, however, that the physics here is more complex than the physics considered by RKKY theory since the hybridization of the As and Mn states plays an essential role in the formation of the induced magnetic moments. In particular, the negative sign of the moment of the As atoms is explained by the property that the empty (hole) states have a large As contribution. Since these states are of the spin-up type the spin-down As states become more occupied than the spin-up ones, leading to a negative induced moment.

#### IV. EXCHANGE PARAMETERS AND CURIE TEMPERATURE

The calculated exchange parameters are presented in Fig. 4. There are a number of conclusions that follow from the analysis of this figure. First, the Heisenberg model with the interaction between the first nearest neighbors only is not able to describe the magnetism of the system. For two Mn concentrations ( $x=25\%$  and  $x=3.125\%$ ) the first nearest-neighbor interaction is even antiferromagnetic; for  $x=12.5\%$  it is positive but small. Second, the exchange interaction is rather quickly decreasing with increasing distance between atoms. In Fig. 4 we show the variation of the Curie temperature ( $T_c$ ) with increasing number of the contributing coordination spheres. For instance, for concentrations  $x=25\%$ ,  $12.5\%$ ,  $6.25\%$  no noticeable contribution to the Curie temperature is obtained from the interactions between Mn atoms at distances larger than  $3a$ . Third, the dependence of the exchange parameters on the distance between Mn atoms is not monotonous. At the distance of  $2a$  the interatomic interaction is negative for all concentrations considered. Although the theory of RKKY interaction is not sufficient to describe the magnetism of the system, it is instructive to compare the characteristic length of the variation of the calculated exchange parameters with the period of the oscillation of the exchange parameters which follows from the RKKY theory. Since the number of holes is exactly one per supercell, the characteristic volume of the Fermi sphere in a simple single-band free-electron model is exactly the volume of the Brillouin zone corresponding to the given supercell. Thus for  $x=25\%$  one can expect oscillations with period close to  $a$  and for  $x=3.125\%$  with period close to  $2a$ . Indeed, analysis of the calculated exchange parameters shows that the first and second oscillations of the exchange parameter for  $x=25\%$  take place at a distance close to  $a$  (from  $1a$  to  $2a$  and from  $2a$  to  $3a$ ). On the other hand, the characteristic range of the variation of the exchange parameter for  $x$

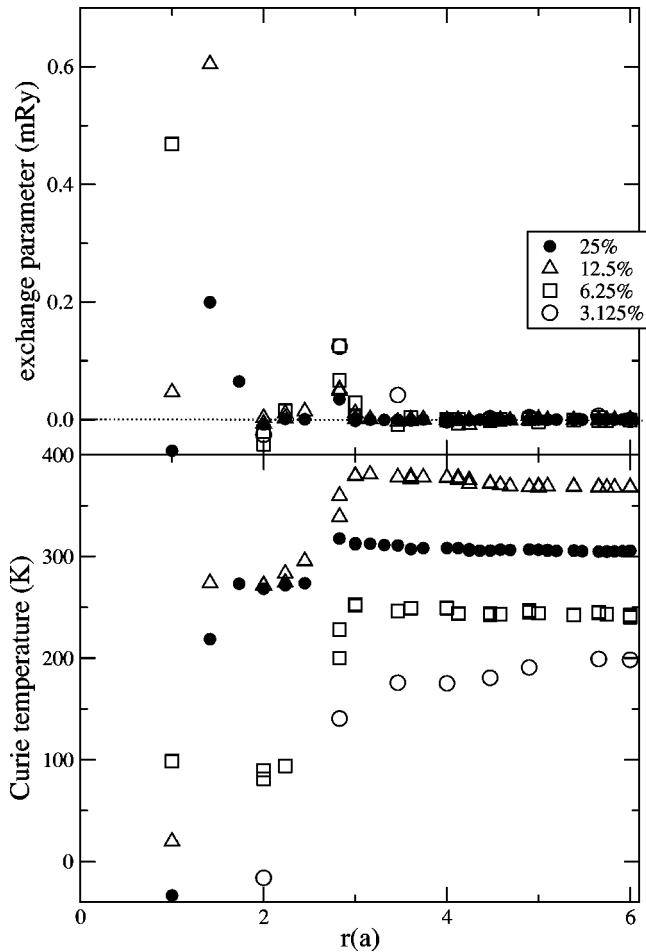


FIG. 4. The parameters of the exchange interaction between Mn atoms (upper panel) and the variation of  $T_C^{MFA}$  with increasing number of the contributing coordination spheres (lower panel). The abscissa gives the radius of the coordination sphere in units of the lattice parameter of the zinc-blende crystal structure.

$= 3.125\%$  is larger (from  $2a$  to  $4a$ ). Thus there is a correlation between the number of holes and the characteristic range of the variation of the exchange parameters.

The calculated Curie temperatures are presented in Fig. 5.

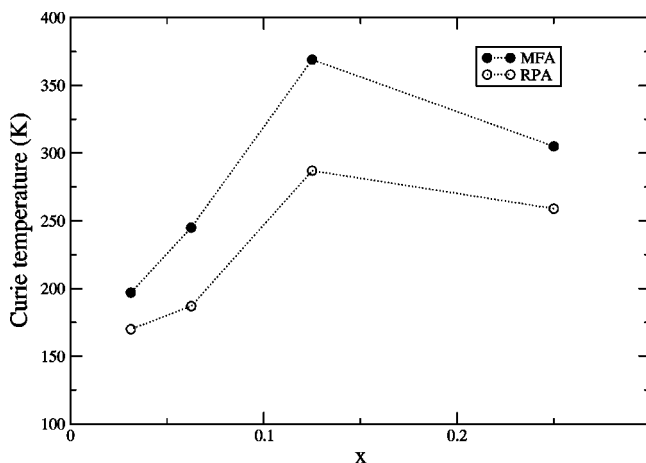


FIG. 5. Curie temperature of  $\text{Ga}_{1-x}\text{Mn}_x\text{As}$ .

Both the MFA and RPA give a similar dependence of the Curie temperature on the Mn concentration: it increases at small  $x$ , has a maximum at  $x = 12.5\%$ , and decreases for higher values of  $x$ . As already stated in Sec. II, the  $T_C^{MFA}$  is always larger than  $T_C^{RPA}$ . However, even  $T_C^{RPA}$  exceeds substantially the experimental values of the transition temperature. A possible explanation of this difference is the presence of As antisites and other donor defects that decrease the concentration of holes in the materials studied experimentally (see, e.g., Refs. 5, 10, and 7). We address this issue in Sec. V.

The nonmonotonous dependence of the transition temperature on the Mn concentration is in qualitative agreement with experiment.<sup>27,29</sup> This nonmonotonous behavior is a consequence of the competition between different trends arising from the increase of the Mn concentration. On the one hand, the amplitude of the effective exchange interaction between the Mn moments through the valence-band states of GaAs increases with decreasing distance between Mn atoms. Also the direct overlap of the Mn states increases. These features produce a trend to increase the Curie temperature with increasing  $x$ . On the other hand, an increased interaction of the states of different Mn atoms results in the broadening of the features of the partial Mn DOS at the Fermi level: As is clearly seen in Fig. 2, at  $x = 3.125\%$  there is a narrow peak at the Fermi energy that is replaced by a broader structure with increasing  $x$ . Simultaneously the Mn magnetic moment decreases (Table I). These properties produce a trend to decrease Curie temperature with increasing Mn concentration.

Interestingly, the induced moment on the nearest As atoms is the same for 25% and 12.5% and decreases for 6.25% and 3.125% although the inducing Mn moment is monotonously increasing (Table I). This shows that the nearest environment of each Mn atom is influenced by other Mn atoms even for the lowest Mn concentration.

## V. DEPENDENCE OF THE CURIE TEMPERATURE ON THE NUMBER OF HOLES

Experimental studies show that the concentration of holes in  $(\text{Ga},\text{Mn})\text{As}$  is lower than the concentration of Mn atoms.<sup>28</sup> One of the important factors leading to the low concentration of holes is the presence of As antisites ( $\text{As}_{\text{Ga}}$ ). Since As has two more valence electrons compared with Ga, each As antisite compensates the holes produced by two Mn atoms.

Here we use a simple rigid-band model to study the dependence of the Curie temperature on the concentration of antisites and other nonmagnetic donors. We assume that the electron structure calculated for  $(\text{Ga},\text{Mn})\text{As}$  with a given Mn concentration will basically be preserved in the presence of defects. The main difference caused by the antisites concerns the occupation of the bands and, respectively, the position of the Fermi level. In Fig. 6 we show the dependence of the Curie temperature calculated in the MFA as a function of the carrier number for  $x = 6.25\%$ . The calculated curve reveals a strong dependence of the Curie temperature on the number of holes in the valence band. In agreement with the commonly accepted picture of hole-mediated ferromagnetism in  $(\text{GaMn})\text{As}$  the decrease of the number of holes leads to a decrease of the Curie temperature. At the number of addi-

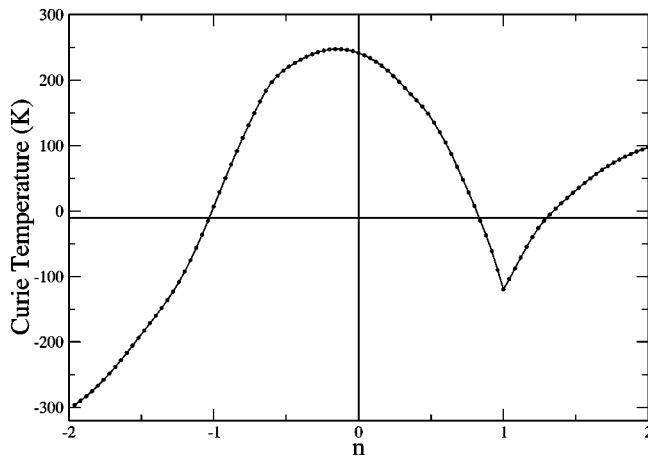


FIG. 6.  $T_C^{MFA}$  for (Ga,Mn)As with Mn concentration  $x = 0.0625$  as a function of the electron number  $n$ . Here  $n=0$  corresponds to the system  $\text{Ga}_{0.9375}\text{Mn}_{0.0625}\text{As}$  with no additional donor or acceptor defects.

tional electrons close to 0.85 (the relation of the hole concentration with respect to the Mn concentration  $p/x=0.15$ ) the ferromagnetic and antiferromagnetic interactions compensate and the value of the mean field acting on the Mn spins in the ferromagnetic state becomes zero. A further decrease of the number of holes leads to negative values of the mean field. The negative value of the Curie temperature in Fig. 6 means that in the assumed ferromagnetic configuration the antiferromagnetic exchange interactions prevail, resulting in a negative exchange field acting on each Mn spin. The ferromagnetic state is unstable.

At  $n=1$  the valence band is full. For larger  $n$  the conduction band is occupied. Discontinuity in the character of the occupied states at  $n=1$  results in a kink in the  $n$  dependence of the value of the mean field. With occupation of the conduction band ( $n>1$ ) the derivative changes sign and the mean field increases with an increase of  $n$ . For the number of electrons in the conduction band larger than 0.28 per Mn atom the mean field becomes positive. Remarkable is the asymmetry of the curve with respect to  $n=1$ . The curve is much steeper to the left from the point than to the right from it. Correspondingly, the Curie temperature at  $n=2$  (one electron in the conduction band per one Mn atom) is about 2.5 times smaller compared to the Curie temperature at  $n=0$  (one hole in the valence band per one Mn atom). This reveals

a higher efficiency of the holes in the valence band in mediating the exchange interaction between the Mn atoms compared with electrons in the conduction band. The physical reason for this property is a stronger exchange interaction between the Mn moments and the states at the top of the valence band ( $p$ - $d$  exchange) compared to the exchange interaction between the Mn moments and the states at the bottom of the conduction band ( $s$ - $d$  exchange).

The region of negative  $n$  (Fig. 6) corresponds to the concentration of holes higher than the concentration of Mn atoms. These states of the system can be obtained by avoiding the formation of  $\text{As}_{\text{Ga}}$  antisites and by codoping with atoms acting as donors. (Of course this simple theoretical consideration does not take into account the difficulties in the producing of materials with such properties.)

Moving in the direction of negative  $n$ , the value of the Curie temperature at first slightly increases. Then the mean-field value decreases fastly revealing again a trend to the antiferromagnetic exchange coupling. The strong dependence of the mean field on the number of carriers reflects the competition between the antiferromagnetic and ferromagnetic interactions.

## VI. CONCLUSIONS

We use supercell and frozen-magnon approaches to study the dependence of the magnetic interactions in (Ga,Mn)As on the Mn concentration. We report the parameters of the exchange interaction between Mn spins and the MFA and RPA estimates of the Curie temperature. In agreement with experiment we obtain a nonmonotonous dependence of the Curie temperature on the Mn concentration. We estimate the dependence of the Curie temperature on the concentration of carries in the system and show that the decrease of the number of holes in the valence band leads to a fast decrease of the Curie temperature. The strong dependence of the Curie temperature on the carrier concentration provides an explanation to the overestimation of the value of the Curie temperature compared to the experiment.

## ACKNOWLEDGMENTS

The financial support of Bundesministerium für Bildung und Forschung is acknowledged. The authors are grateful to J. Kudrnovsky for interesting discussions and A. Ernst for sharing with us his computer subroutines.

\*Electronic address: lsandr@mpi-halle.de

<sup>1</sup>H. Ohno, H. Munekata, T. Penney, S. von Molnar, and L.L. Chang, Phys. Rev. Lett. **68**, 2664 (1992).

<sup>2</sup>H. Ohno, A. Shen, F. Matsukura, A. Oiwa, A. Endo, and S. Kusunoto, Appl. Phys. Lett. **69**, 363 (1996).

<sup>3</sup>T. Dietl, Semicond. Sci. Technol. **17**, 377 (2002).

<sup>4</sup>J. König, J. Schliemann, T. Jungwirth, and A.H. MacDonald, cond-mat/0111314 (unpublished).

<sup>5</sup>H. Akai, Phys. Rev. Lett. **81**, 3002 (1998).

<sup>6</sup>K. Sato and H. Katayama-Yosida, Semicond. Sci. Technol. **17**, 367 (2002).

<sup>7</sup>P.A. Korzhavii, I.A. Abrikosov, E.A. Smirnova, L. Bergqvist, P.

Mohn, R. Mathieu, P. Svedlindh, J. Sadowski, E.I. Isaev, Yu.Kh. Vekilov, and O. Eriksson, Phys. Rev. Lett. **88**, 187202 (2002).

<sup>8</sup>Y.-J. Zhao, W.T. Geng, K.T. Park, and A.J. Freeman, Phys. Rev. B **64**, 035207 (2001).

<sup>9</sup>S. Sanvito, P. Ordejon, and N.A. Hill, Phys. Rev. B **63**, 165206 (2001).

<sup>10</sup>S. Sanvito and N.A. Hill, Appl. Phys. Lett. **78**, 3493 (2001).

<sup>11</sup>M. van Schilfgarde and O.N. Mryasov, Phys. Rev. B **63**, 233205 (2001).

<sup>12</sup>*Electronic Structure and Physical Properties of Solids*, edited by H. Dreyse (Springer, Berlin, 2000).

<sup>13</sup>A.I. Liechtenstein, M.I. Katsnelson, V.P. Antropov, and V.A.

- Gubanov, J. *Magn. Magn. Mater.* **67**, 65 (1987).
- <sup>14</sup>M. Uhl and J. Kübler, *Phys. Rev. Lett.* **77**, 334 (1996).
- <sup>15</sup>N.M. Rosengaard and B. Johansson, *Phys. Rev.* **55**, 14 975 (1997).
- <sup>16</sup>S.V. Halilov, H. Eschrig, A.Y. Perlov, and P.M. Oppeneer, *Phys. Rev. B* **58**, 293 (1998).
- <sup>17</sup>Q. Niu and L. Kleinman, *Phys. Rev. Lett.* **80**, 2205 (1998).
- <sup>18</sup>S.Y. Savrasov, *Phys. Rev. Lett.* **81**, 2570 (1998).
- <sup>19</sup>R.H. Brown, D.M.C. Nicholson, X. Wang, and T.C. Schulthess, *J. Appl. Phys.* **85**, 4830 (1999).
- <sup>20</sup>M. Pajda, J. Kudrnovsky, I. Turek, V. Drchal, and P. Bruno, *Phys. Rev. B* **64**, 174402 (2001).
- <sup>21</sup>O. Grotheer, C. Ederer, and M. Fähnle, *Phys. Rev. B* **63**, 100401 (2001).
- <sup>22</sup>T. Moriya, *Spin Fluctuations in Itinerant Electron Magnetism* (Springer, Berlin, 1985).
- <sup>23</sup>C. Herring, in *Magnetism IV*, edited by G. Rado and H. Suhl (Academic Press, New York, 1966).
- <sup>24</sup>L.M. Sandratskii, *Phys. Status Solidi B* **135**, 167 (1986).
- <sup>25</sup>A.R. Williams, J. Kübler, and C.D. Gelatt, *Phys. Rev. B* **19**, 6094 (1979).
- <sup>26</sup>G. Schmidt, D. Ferrand, L.W. Molenkamp, A.T. Filip, and B.J. van Wees, *Phys. Rev. B* **62**, 4790 (2000).
- <sup>27</sup>F. Matsukura, H. Ohno, A. Shen, and Y. Sugawara, *Phys. Rev. B* **57**, 2037 (1998).
- <sup>28</sup>H. Ohno, *J. Magn. Magn. Mater.* **200**, 110 (1999).
- <sup>29</sup>The maximum in the experimental dependence of the Curie temperature on the Mn concentration is at  $x$  about 5%, which is substantially smaller than the theoretical value. A similar result was obtained by Kudrnovsky (Ref. 30) within the CPA calculation. Our preliminary results within the approach discussed in Sec. V show that the account for As antisites shifts the position of the maximum to smaller  $x$ .
- <sup>30</sup>J. Kudrnovsky (private communication).